

Polar-Nematic Order at the Interface of Motility-Induced Phase Separation: The Importance of Looking Ahead

Chiu Fan Lee*

*Department of Bioengineering, Imperial College London,
South Kensington Campus, London SW7 2AZ, U.K.*

Motility-induced phase separation is a purely non-equilibrium phenomenon in which self-propelled particles aggregate without any attractive interactions. One surprising feature of MIPS is the emergence of polar-nematic order at the interfacial region, whose underlying physics remains poorly understood. Here, I will show analytically and numerically that the many-body physics leading to the interfacial ordering behavior can be captured by an effective speed model. In this model, each particle's speed depends on the system's density a short distance ahead of its direction of motion.

The study of active matter is crucial to our understanding of diverse living matter and driven synthetic systems [1, 2]. In addition to being paramount to our quantitative description of various natural and artificial phenomena, much novel universal behavior has also been uncovered in active matter systems in the hydrodynamic limits, which ranges from novel phases [3–10] to critical phenomena [11–14]. Besides the hydrodynamic limits, interesting emergent phenomena also occur in the microscopic and mesoscopic scales. In the case of motility-induced phase separation (MIPS) [15–19], one of these emergent phenomena is the polar-nematic ordering behavior at the liquid-gas interface (Fig. 1) [20–23]. Understanding this phenomenon will be integral to modeling quantitatively diverse interface-related properties of MIPS that include nucleation [24], wetting [25, 26], negative interfacial tension [27–29], and reverse Ostwald ripening [30, 31].

Although the interfacial polar-nematic order ultimately emerges from the many-body interactions of the system, similar ordering pattern in fact already occurs in a system of *non-interacting* self-propelled particles (i.e., an ideal active gas) around an impenetrable wall – particles stuck at the wall tend to point towards it (hence the system is polar), and particles right outside the wall are predominantly moving parallel to the wall (hence nematic), since they constitute particles whose orientations have just rotated enough to be pointing away from the wall [32, 33]. This revelation suggests that the polar-nematic pattern observed in MIPS can be studied using an effective model in which all particle-particle interactions are simply captured by a speed function that depends purely on the system's local configurations. For instance, each particle's speed can depend solely on the system's density at its present location. The first surprising finding of this work is a demonstration that such a model, although capable of exhibiting MIPS, cannot account for the polar-nematic pattern at the interface. I will then show that incorporating the finite size of the particles into the model in a minimal way is sufficient to capture the interfacial ordering behavior. Specifically, instead of having the particle's speed dependent on the system's density at the particle's position, the speed de-

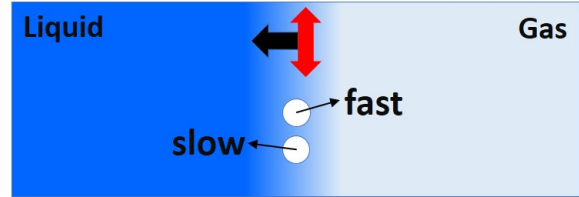


FIG. 1. Schematic of the generic polar-nematic ordering at the interface of MIPS. The shade of blue depicts the density of the system. The particles' orientations are isotropic in the bulks of both liquid and gas phases. As one approaches the interface from the liquid phase, the average orientation of the particles at the interfacial region becomes polar (pointing towards the liquid phase as indicated by the black arrow), and then nematic (i.e., particles' orientations tend to be approximately vertical, as indicated by the red double-arrow.) The emergence of the polar-nematic order can be captured by an effective speed model in which each particle's speed depends on the system's density a short distance (e.g., by a distance corresponding to the radius of particle) ahead of its direction of motion. For instance, a particle in the interfacial region moving towards the gas phase (top white circle) is faster than another particle with the same center of mass position but moving towards the more condensed liquid phase (bottom white circle).

pends on the density a short distance (e.g., the radius of the particle) ahead of the particle's orientation. This assumption can be easily motivated by the expectation that a particle going into a dense environment will be slower than one going into emptier space (Fig. 1). Indeed, a single self-propelled hard sphere of radius a that is a distance a away from an impenetrable wall will have a speed of zero if its orientation is pointing into the wall, while its speed will be non-zero if it is pointing away from the wall. In the following, I will first proceed analytically and then illustrate all findings numerically.

Analytical argument.—In two dimensions, an archetype of active systems exhibiting MIPS consists of a collection of N polar self-propelled particles in a finite volume V , such that the particles interact purely sterically via a short-ranged repulsive potential energy

U , whose exact form is unimportant. Each particle also exerts a constant active force, f_a , that points to a particular orientation denoted by $\hat{\mathbf{n}} \equiv \cos \Theta \hat{\mathbf{x}} + \sin \Theta \hat{\mathbf{y}}$, and the angle Θ itself undergoes diffusion with the rotational diffusion coefficient D_r . Hence, the microscopic equations of motion (EOM) of the system are

$$\frac{d\mathbf{R}_i}{dt} = -\frac{1}{\eta} \sum_{j \neq i} \nabla_{\mathbf{R}_i} U(|\mathbf{R}_i - \mathbf{R}_j|) + \frac{f_a}{\eta} \hat{\mathbf{n}}_i \quad (1a)$$

$$\frac{d\Theta_i}{dt} = \sqrt{2D_r} g_i(t), \quad (1b)$$

where the indices i, j enumerate the particles ($i, j = 1, 2, \dots, N$), $\mathbf{R}_i(t)$ is the i -th particle's position at time t , η is the damping coefficient in this over-damped system, and $g_i(t)$ denotes Gaussian noise terms such that $\langle g_i(t) \rangle = 0$ and $\langle g_i(t) g_j(t') \rangle = \delta_{ij} \delta(t - t')$.

Since the particles' identities are irrelevant, we can focus instead on the temporal evolution of the N -particle density function:

$$\psi(\mathbf{r}, \theta, t) = \sum_{i=1}^N \delta^2(\mathbf{r} - \mathbf{R}_i(t)) \delta(\theta - \Theta_i(t)), \quad (2)$$

whose EOM can be constructed from the microscopic EOM (1) (see, e.g., [22]).

As mentioned in the introduction, the goal here is to account for all particle-particle interactions and fluctuations through an effective speed that depends on the density of the system a distance a ahead in the orientation of the particle under consideration. Specifically, the effective EOM of ψ is of the form:

$$\partial_t \psi = -\nabla \cdot \left[v \left(\rho(\mathbf{r} + a\hat{\mathbf{n}}, t) \right) \hat{\mathbf{n}} \psi \right] + D_r \partial_\theta^2 \psi, \quad (3)$$

where $\rho(\mathbf{r}, t) = \int d\theta \psi(\mathbf{r}, \theta, t)$ is the density, and $v(\rho)$ is an effective speed that decreases monotonically as ρ increases.

To make analytical progress, I will further assume that a is small and make the following approximation:

$$v(\rho(\mathbf{r} + a\hat{\mathbf{n}}, t)) \approx v(\rho(\mathbf{r}, t)) + a \left. \frac{dv}{d\rho} \right|_{\rho(\mathbf{r}, t)} \hat{\mathbf{n}} \cdot \nabla \rho(\mathbf{r}, t). \quad (4)$$

With this simplification, we are now ready to systematically construct a reduced set of EOM in which the fields of interest depend on \mathbf{r} and t , but not θ . Specifically, these fields will be M -th rank tensors of the form: $\int d\theta \hat{n}_{\alpha_1} \hat{n}_{\alpha_2} \dots \hat{n}_{\alpha_M} (\psi - \rho/(2\pi))$, where the Greek letters enumerate the spatial coordinates and the subtraction of $\rho/(2\pi)$ in the definition ensures that these tensor fields vanish if ψ is isotropic in θ . For instance, the *unnormalized* polar field $\mathbf{m}(\mathbf{r}, t)$ and nematic field \mathbf{Q} are the first-rank and second-rank tensors, respectively:

$$m_\alpha = \int d\theta \hat{n}_\alpha \psi, \quad Q_{\alpha\beta} = \int d\theta \left(\hat{n}_\alpha \hat{n}_\beta - \frac{\delta_{\alpha\beta}}{2} \right) \psi. \quad (5)$$

These fields are unnormalized since their norms are not between 0 and 1, as opposed to, e.g., the normalized polar field $\mathbf{m}^N = \rho^{-1} \int d\theta \hat{\mathbf{n}} \psi$.

From (3), the EOM of these two fields are:

$$\partial_t \rho = -\partial_\alpha \left[v(\rho) m_\alpha + a \frac{dv}{d\rho} (\partial_\beta \rho) \left(Q_{\alpha\beta} + \frac{\delta_{\alpha\beta} \rho}{2} \right) \right] \quad (6a)$$

$$\begin{aligned} \partial_t m_\alpha = & -\partial_\beta \left[v(\rho) \left(Q_{\alpha\beta} + \frac{\delta_{\alpha\beta} \rho}{2} \right) + a \frac{dv}{d\rho} (\partial_\gamma \rho) R_{\alpha\beta\gamma} \right] \\ & - D_r m_\alpha, \end{aligned} \quad (6b)$$

where $\partial_\alpha \equiv \partial/\partial r_\alpha$ and repeated indices are summed over. The unnormalized tetrahedral tensor field $R_{\alpha\beta\gamma} = \int d\theta \hat{n}_\alpha \hat{n}_\beta \hat{n}_\gamma \psi$ was also introduced in (6). The EOM of higher-rank tensor fields can be derived similarly, and the EOM of the M -th rank tensor field will involve the $(M+1)$ -th rank and $(M+2)$ -th rank tensor fields.

Without loss of generality, I will from now assume that there is a single vertical interface located at around $x = 0$ in this phase separated system. Hence, all fields at the steady state vary only with the x coordinate. As a result, $m_y = 0$, $Q_{xy} = Q_{yx} = 0$, and the nematic scalar order parameter S is identical to $|Q_{xx}^N|$ where $\mathbf{Q}^N = 2\rho^{-1} \mathbf{Q}$ is the normalized nematic \mathbf{Q} -tensor.

Let us now first focus on the case of $a = 0$, i.e., the particle's speed depends only on the density at its center of mass position. At the steady-state, (6) become simply:

$$\frac{d}{dx} [v(\rho) m_\alpha] = 0 \quad (7a)$$

$$\frac{d}{dx} \left[v(\rho) \left(Q_{xx} + \frac{\rho}{2} \right) \right] + D_r m_x = 0. \quad (7b)$$

A solution to the above equations can be easily obtained by inspection: $m_x = Q_{xx} = 0$ and $\rho(x) \propto [v(\rho(x))]^{-1}$. Namely, the density is high wherever $v(\rho(x))$ is low and vice versa. Therefore, this model can account for phase separation (e.g., when the speed function v is a monotonically decreasing and sigmoidal-like function of ρ), but is incapable of exhibiting polar-nematic order at the interface since m_x and Q_{xx} are identically zero. Incorporating higher-order tensor fields into the consideration will not alter this conclusion. Indeed, this result can also be derived directly from (3) by assuming that $a = 0$ and ψ is isotropic in θ . In summary, an effective speed model without *looking ahead* cannot capture the interfacial ordering behavior. I will confirm this prediction numerically in the next section.

Let us now restore the "looking ahead" feature into the model by making a non-zero. To make analytical progress, I will set $R_{\alpha\beta\gamma}$ and all higher rank tensor fields to zero. Note that since $|\hat{\mathbf{n}}| \leq 1$, the entries in higher rank tensor fields are generically expected to be smaller than those of lower rank tensor fields. However, setting R and other higher rank tensor fields to zero is still an

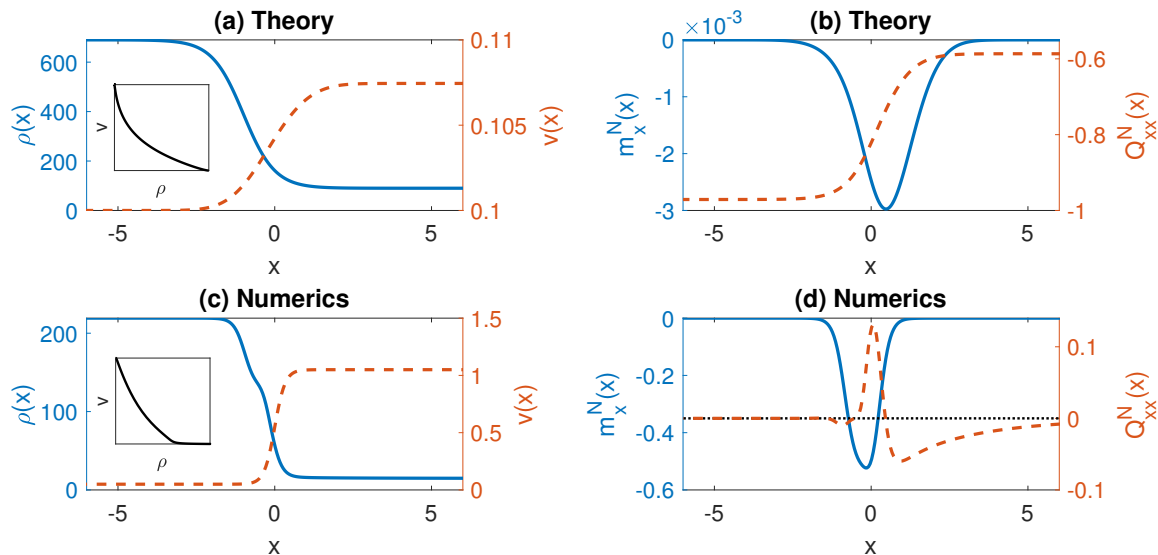


FIG. 2. System's configurations at the MIPS interface. (a) & (c) The interface is around $x = 0$ with the liquid phase (high density ρ and slow particles' speed v) to the left and the gas phase (low ρ and fast speed v) to the right. The inset plots show how the speed function v decays with ρ . (b) & (d) The normalized polarization m_x^N is peaked at around the interface, while the nematic order is negative to the right of the m_x^N peak. A negative Q_{xx}^N means that the average orientation of the particles are more vertical than horizontal, and vice versa. The fact that the scalar nematic order, $S = |Q_{xx}^N|$, does not decay to zero away from the interface in (b) is an artefact of the approximation made to make analytical progress, and it does decay to zero in the numerical study of the full effective model (3) shown in (d). For (c) and (d), the x -axis is shifted so that the interface is around $x = 0$.

uncontrolled approximation, but it is one that can be systematically improved upon in future work.

With this additional approximation, the steady-state equations (6) are now

$$vm_x + a \frac{dv}{dx} \left(Q_{xx} + \frac{\rho}{2} \right) = 0 \quad (8a)$$

$$\frac{d}{dx} \left[v \left(Q_{xx} + \frac{\rho}{2} \right) \right] + D_r m_x = 0. \quad (8b)$$

In (8a), I have used the fact that $(dv/d\rho)(d\rho/dx) = dv/dx$.

Using (8a), we have

$$Q_{xx} + \frac{\rho}{2} = -\frac{vm_x}{a(dv/dx)}. \quad (9)$$

Substituting this into (8b), and letting $I(x) = \int_{-\infty}^x m_x(x') dx'$, we have

$$D_r I(x) = \frac{v^2 m_x}{a(dv/dx)} - A, \quad (10)$$

where $A = \frac{v^2 m_x}{a(dv/dx)} \Big|_{x \rightarrow -\infty}$. Note that although we expect both m_x and dv/dx to go to zero as $x \rightarrow -\infty$, their ratio does not have to vanish in this limit. Indeed, given that the liquid phase is on the left, we expect that $m_x < 0$ (since the polar field points to the liquid phase)

and $dv/dx > 0$ (since the speed goes down with density, which is monotonically increasing with x), hence A is expected to be negative.

The solution to the differential equation (10) is

$$v(x) = \left[\frac{1}{v_c} - \frac{1}{aD_r} \ln \left| \frac{D_r I(x) + A}{A} \right| \right]^{-1}, \quad (11)$$

where $v_c = v|_{x \rightarrow -\infty}$.

I will now construct a particular example that exhibits the expected interfacial ordering. Since we expect the polar order to be negative and peaked at the interface [20–23], I will let

$$m_x(x) = -\frac{1}{\sqrt{2\pi}} e^{-x^2/2}. \quad (12)$$

Given the above expression of m_x ,

$$I(x) = -\frac{1}{2} \left[1 + \operatorname{erf} \left(\frac{x}{\sqrt{2}} \right) \right], \quad (13)$$

and v is then defined via (11). Using (9), we can further determine $Q_{xx} + \rho/2$, but *not* Q_{xx} and ρ individually. This peculiar non-uniqueness is of course due to the uncontrolled approximation adopted. As a result, the density variation $\rho(x)$ can be chosen arbitrarily, subject to i) it is monotonically decreasing, and ii) both the normalized polarization vector field $|\mathbf{m}^N|$ and the normalized

nematic scalar order parameter $S = |Q_{xx}^N|$ are between 0 and 1 for all x .

A particular realization is illustrated in Fig. 2, with $a = 1$, $A = -1$, $D_r = 1$, $v_c = 1/10$, and $\rho(x)$ is defined to be $60 \times (1.35 - \tanh(x+1))$. Although key interfacial features are captured in this model, the nematic order remains high away from the interface, contrary to known simulation results showing that \mathbf{Q} decays to zero from the interface [20–23]. This discrepancy is an artefact of the severe approximations made to make analytical progress (i.e., a is small and the neglect of higher rank tensor fields in the EOM). Indeed, I will now turn to simulation to show that the underlying physics of MIPS interfacial ordering can indeed be captured by the effective speed model introduced in (3).

Numerical results.—To show the emergence of interfacial polar-nematic order in MIPS, I will first assign a spatially varying, sigmoidal-like speed function in (3), and then obtain the resulting steady-state density function and polar-nematic pattern numerically. The actual speed-density relationship can then be inferred from the steady-state configuration.

For computational efficiency, I will solve for the steady state of ψ (3) using a scheme akin to lattice Boltzmann methods (LBM) [34, 35], albeit one tailored for dry active matter [36]. Specifically, I first discretize both space and angular orientations and denote $\psi(x_i, \theta_j, t)$ by $P_{ij}(t)/(\Delta\theta\Delta x)$ where $\theta_j = 2\pi(j+1/2)/N_\theta$, $j = 0, 1, \dots, N_\theta - 1$, and $x_i = i\Delta x/L$, $i = 1, \dots, N_x$. The temporal evolution of P_{ij} then consists of i) a streaming step:

$$(1 - u_{ij})P_{ij} + \sum_{e=\pm 1} H(e \cos \theta_j) u_{i-e, j} P_{i-e, j} \mapsto P_{ij}, \quad (14)$$

where $H(\cdot)$ is the Heaviside function and

$$u_{ij} = v(x_i + a \cos \theta_j) |\cos \theta_j| \Delta t, \quad (15)$$

where v is a prescribed spatially varying speed function; and ii) an on-site re-distribution step that corresponds to rotational diffusion:

$$(1 - 2\alpha)P_{ij}(t) + \alpha \sum_{e=\pm 1} P_{i, \text{mod}_{N_\theta}(j+e)}(t) \mapsto P_{ij}, \quad (16)$$

where $\alpha = N_\theta^2/(2\pi)^2 D_r \Delta t$. The spatial boundary condition in the streaming step is the reflective boundary condition (i.e., $P_{1j} \mapsto P_{1, \text{mod}_{N_\theta}(j+N_\theta/2)}$ if $\pi/2 < \theta_j < 3\pi/2$, and $P_{N_x, j} \mapsto P_{N_x, \text{mod}_{N_\theta}(j+N_\theta/2)}$ if $-\pi/2 < \theta_j < \pi/2$). Steps i) and ii) are then repeated until the maximal incremental change, $\max_{i,j} |\Delta P_{ij}|$, is below certain threshold.

In the numerical scheme, the spatially varying speed function $v(x)$ is prescribed to be $[\tanh(3x - L) + 1.1]/2$. The physical dependency of v on ρ can then be obtained by relating the density variation with the speed variation at the steady state (inset of Fig. 2(c)). The other

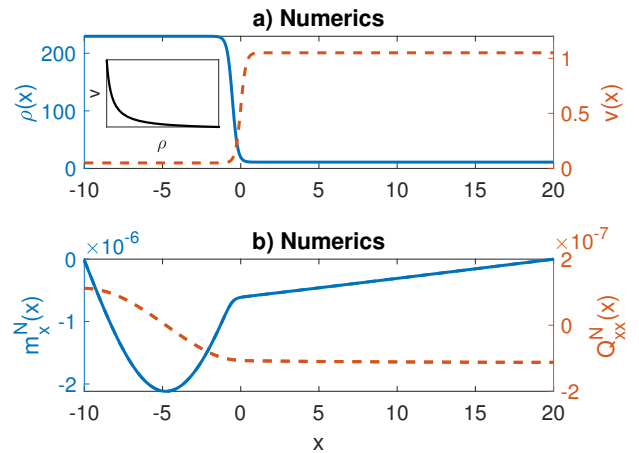


FIG. 3. System's configuration when each particle's speed depends only on the system's density at their center of mass (i.e., $a = 0$ in (15)). (a) & (b) correspond to Fig. 2(a) & (c), respectively. The small values of m_x^N and Q_{xx}^N stem from boundary effects and are negligible compared to those in Fig. 2.

parameters are: $a = 0.5$, $\alpha = 0.3$, $N_\theta = 80$, $N_x = 600$, $L = 30$, and $\Delta t = 0.02$. Other values of N_x and N_θ were also studied, but the results remain qualitatively the same. The numerical procedure starts with uniform $P_{ij} = 1/2$ and stops when $\max_{i,j} |\Delta P_{ij}| < 10^{-10}$ (with a total temporal evolution of around $3 \times 10^6 \Delta t$).

The numerical results are shown in Figs 2(c) & (d), demonstrating the expected polar-nematic order at the interface, thus validating that the effective speed model proposed in (3) captures the characteristic interfacial ordering in MIPS.

By repeating the simulation protocol with a set to zero in (15), Fig. 3 shows that the numerical results are consistent with the previous analytical prediction – phase separation is possible in this case (Fig. 3(a)), but interfacial ordering cannot exist (Fig. 3(b)).

Summary & Outlook.— I have demonstrated, analytically and numerically, that the emergence of polar-nematic order at the liquid-gas interface of MIPS can be captured by an effective speed model in which each particle's speed depends on the density of the system ahead of the particle's orientation. On the analytical side, there is still some discrepancy with regards to the spatial variation of nematic tensor field, and systematic improvement upon the current work would constitute an interesting future direction. Other interesting directions include the quantification of how the interfacial ordering impacts upon other interface-related phenomena in MIPS that include the Gibbs-Thomson relation [20], wetting [25, 26], and reverse Ostwald ripening [30, 31].

-
- * c.lee@imperial.ac.uk
- [1] M C Marchetti, J F Joanny, S Ramaswamy, T B Liverpool, J Prost, Madan Rao, and R Aditi Simha, “Hydrodynamics of soft active matter,” *Reviews of Modern Physics* **85**, 1143–1189 (2013).
 - [2] Daniel Needleman and Zvonimir Dogic, “Active matter at the interface between materials science and cell biology,” *Nature Reviews Materials* **2**, 17048 (2017).
 - [3] Tamás Vicsek, András Czirók, Eshel Ben-Jacob, Inon Cohen, and Ofer Shochet, “Novel Type of Phase Transition in a System of Self-Driven Particles,” *Physical Review Letters* **75**, 1226–1229 (1995).
 - [4] John Toner and Yuhai Tu, “Long-Range Order in a Two-Dimensional Dynamical XY Model: How Birds Fly Together,” *Physical Review Letters* **75**, 4326–4329 (1995).
 - [5] John Toner and Yuhai Tu, “Flocks, herds, and schools: A quantitative theory of flocking,” *Physical Review E* **58**, 4828–4858 (1998).
 - [6] John Toner, “Birth, Death, and Flight: A Theory of Malthusian Flocks,” *Physical Review Letters* **108**, 088102 (2012).
 - [7] Leiming Chen, Chiu Fan Lee, and John Toner, “Incompressible polar active fluids in the moving phase in dimensions $d > 2$,” *New Journal of Physics* **20**, 113035 (2018).
 - [8] Benoît Mahault, Francesco Ginelli, and Hugues Chaté, “Quantitative Assessment of the Toner and Tu Theory of Polar Flocks,” *Physical Review Letters* **123**, 218001 (2019).
 - [9] Leiming Chen, Chiu Fan Lee, and John Toner, “Moving, Reproducing, and Dying Beyond Flatland: Malthusian Flocks in Dimensions $d > 2$,” *Physical Review Letters* **125**, 098003 (2020), arXiv:2001.01300.
 - [10] Leiming Chen, Chiu Fan Lee, and John Toner, “A novel nonequilibrium state of matter: a $d = 4 - \epsilon$ expansion study of Malthusian flocks,” (2020), arXiv:2004.00129.
 - [11] Francesco Ginelli and Hugues Chaté, “Relevance of Metric-Free Interactions in Flocking Phenomena,” *Physical Review Letters* **105**, 168103 (2010), arXiv:1007.1783.
 - [12] Anton Peshkov, Sandrine Ngo, Eric Bertin, Hugues Chaté, and Francesco Ginelli, “Continuous Theory of Active Matter Systems with Metric-Free Interactions,” *Physical Review Letters* **109**, 098101 (2012).
 - [13] Leiming Chen, John Toner, and Chiu Fan Lee, “Critical phenomenon of the order-disorder transition in incompressible active fluids,” *New Journal of Physics* **17**, 042002 (2015).
 - [14] B. Mahault, X.-c. Jiang, E. Bertin, Y.-q. Ma, A. Patelli, X.-q. Shi, and H. Chaté, “Self-Propelled Particles with Velocity Reversals and Ferromagnetic Alignment: Active Matter Class with Second-Order Transition to Quasi-Long-Range Polar Order,” *Physical Review Letters* **120**, 258002 (2018), arXiv:1803.00104.
 - [15] Yaouen Fily and M Cristina Marchetti, “Athermal Phase Separation of Self-Propelled Particles with No Alignment,” *Physical Review Letters* **108**, 235702 (2012).
 - [16] Gabriel S Redner, Michael F Hagan, and Aparna Baskaran, “Structure and Dynamics of a Phase-Separating Active Colloidal Fluid,” *Physical Review Letters* **110**, 055701 (2013).
 - [17] J Tailleur and M E Cates, “Statistical Mechanics of Interacting Run-and-Tumble Bacteria,” *Physical Review Letters* **100**, 218103 (2008).
 - [18] Michael E Cates and Julien Tailleur, “Motility-Induced Phase Separation,” *Annual Review of Condensed Matter Physics* **6**, 219–244 (2015).
 - [19] M. Cristina Marchetti, Yaouen Fily, Silke Henkes, Adam Patch, and David Yllanes, “Minimal model of active colloids highlights the role of mechanical interactions in controlling the emergent behavior of active matter,” *Current Opinion in Colloid & Interface Science* **21**, 34–43 (2016), arXiv:1510.00425.
 - [20] Chiu Fan Lee, “Interface stability, interface fluctuations, and the Gibbs–Thomson relationship in motility-induced phase separations,” *Soft Matter* **13**, 376–385 (2017).
 - [21] Adam Patch, Daniel M. Sussman, David Yllanes, and M. Cristina Marchetti, “Curvature-dependent tension and tangential flows at the interface of motility-induced phases,” *Soft Matter* **14**, 7435–7445 (2018), arXiv:1804.06838.
 - [22] Alexandre P Solon, Joakim Stenhammar, Michael E Cates, Yariv Kafri, and Julien Tailleur, “Generalized thermodynamics of motility-induced phase separation: phase equilibria, Laplace pressure, and change of ensembles,” *New Journal of Physics* **20**, 075001 (2018).
 - [23] Ahmad K. Omar, Zhen Gang Wang, and John F. Brady, “Microscopic origins of the swim pressure and the anomalous surface tension of active matter,” *Physical Review E* **101**, 012604 (2020), arXiv:1912.11727.
 - [24] Gabriel S. Redner, Caleb G. Wagner, Aparna Baskaran, and Michael F. Hagan, “Classical Nucleation Theory Description of Active Colloid Assembly,” *Physical Review Letters* **117**, 148002 (2016).
 - [25] Adam Wysocki and Heiko Rieger, “Capillary Action in Scalar Active Matter,” *Physical Review Letters* **124**, 048001 (2020), arXiv:1908.03368.
 - [26] Pedro D. Neta, Mykola Tasinkevych, Margarida M. Telo da Gama, and Cristóvão S. Dias, “Wetting of a solid surface by active matter,” *Soft Matter* **17**, 2468–2478 (2021), arXiv:2011.05963.
 - [27] Julian Bialké, Jonathan T Siebert, Hartmut Löwen, and Thomas Speck, “Negative Interfacial Tension in Phase-Separated Active Brownian Particles,” *Physical Review Letters* **115**, 098301 (2015).
 - [28] Siddharth Paliwal, Vasileios Prymidis, Laura Fillion, and Marjolein Dijkstra, “Non-Equilibrium Surface Tension of the Vapour-Liquid Interface of Active Lennard-Jones Particles,” *Journal of Chemical Physics* **147**, 084902 (2017), arXiv:1706.03007.
 - [29] Alternative formulation of the surface tension different from the generalized Irving-Kirkwood approach has also been proposed: Sophie Hermann, Daniel de las Heras, and Matthias Schmidt, “Non-negative Interfacial Tension in Phase-Separated Active Brownian Particles,” *Physical Review Letters* **123**, 268002 (2019).
 - [30] Elsen Tjhung, Cesare Nardini, and Michael E. Cates, “Cluster Phases and Bubbly Phase Separation in Active Fluids: Reversal of the Ostwald Process,” *Physical Review X* **8**, 031080 (2018).
 - [31] Giordano Fausti, Elsen Tjhung, Michael Cates, and Cesare Nardini, “Capillary interfacial tension in active phase separation,” (2021), arXiv:2103.15563.
 - [32] Chiu Fan Lee, “Active particles under confinement: Aggregation at the wall and gradient formation inside a channel,” *New Journal of Physics* **15**, 055007 (2013).

- [33] Caleb G. Wagner, Michael F. Hagan, and Aparna Baskaran, “Steady-state distributions of ideal active Brownian particles under confinement and forcing,” *Journal of Statistical Mechanics: Theory and Experiment* **2017**, 043203 (2017), arXiv:1611.01834.
- [34] S Succi, *The Lattice Boltzmann Equation: For Fluid Dynamics and Beyond*, Numerical Mathematics and Scientific Computation (Clarendon Press, 2001).
- [35] Timm Krüger, Halim Kusumaatmaja, Alexandr Kuzmin, Orest Shardt, Goncalo Silva, and Erlend Magnus Viggen, *The Lattice Boltzmann Method*, Graduate Texts in Physics (Springer International Publishing, Cham, 2017).
- [36] David Nesbitt, Gunnar Pruessner, and Chiu Fan Lee, “Uncovering novel phase transitions in dense dry polar active fluids using a lattice Boltzmann method,” *New Journal of Physics* (2021), 10.1088/1367-2630/abd8c0, arXiv:1902.00530.